

Supplementary Materials for **Emergence of Kondo lattice behavior in a van der Waals itinerant ferromagnet, Fe₃GeTe₂**

Yun Zhang, Haiyan Lu, Xiegang Zhu, Shiyong Tan, Wei Feng, Qin Liu, Wen Zhang, Qiuyun Chen, Yi Liu,
Xuebing Luo, Donghua Xie, Lizhu Luo, Zhengjun Zhang, Xinchun Lai

Published 12 January 2018, *Sci. Adv.* **4**, eaao6791 (2018)
DOI: 10.1126/sciadv.aao6791

This PDF file includes:

- fig. S1. Hysteresis loop for H parallel to the c axis at 2 K.
- fig. S2. Spectral weight transfer at other momentum locations.
- fig. S3. Enlarged Fermi surface volume in the FM state.
- fig. S4. Spatial-resolved low-energy dI/dV spectra at different temperatures.
- fig. S5. Band structures of Te-terminated FGT in the PM state.
- fig. S6. The positive correlation between ferromagnetism and Kondo lattice behavior.
- References (53–65)

Supplementary Materials

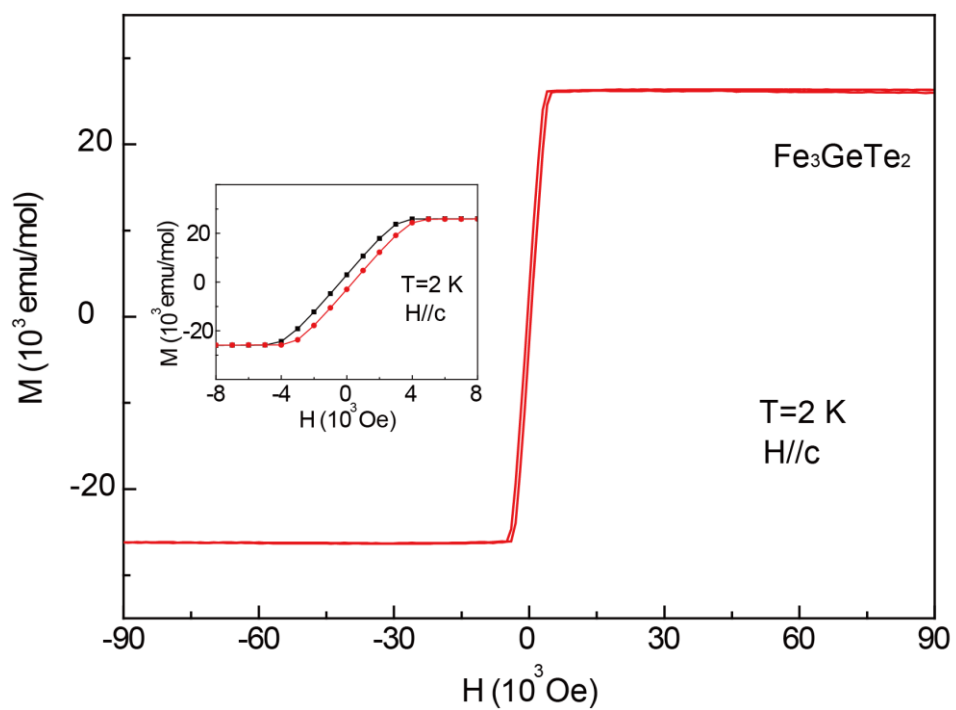


fig. S1. Hysteresis loop for H parallel to the c axis at 2 K. The loop indicates that the ground state of FGT is ferromagnetic. Insert shows the low magnetic field section.

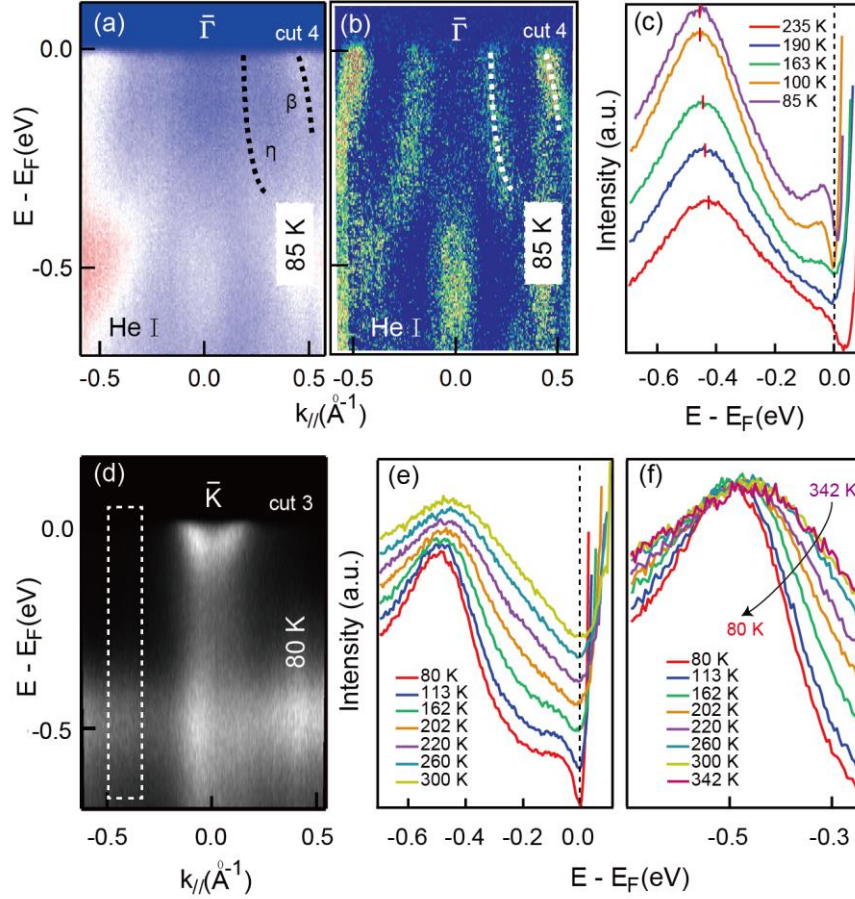


fig. S2. Spectral weight transfer at other momentum locations. (a and b) Photoemission intensity plot and the corresponding curvature intensity plot with He I light at 85 K along cut 4 in Fig. 3(a) in the main text. The dashed lines trace the main valence bands. (c) The AIPES data of valence band in fig. S2(a) divided by the Fermi-Dirac function at different temperatures. (d) Photoemission intensity plot of γ band with He I light at 85 K. (e) The AIPES data of the band structure in fig. S2(d) divided by the Fermi-Dirac function at different temperatures. The integrated range is marked by the dashed rectangle in fig. S2(d). (f) Amplified AIPES data in fig. S2(e). The intensities are normalized at 500 meV BE. A similar redistribution of the spectral weight to γ band is observed at other momentum positions in fig. S2(c) and (e). When the temperature decreases, several features appear. 1) a peak centred at 50 meV BE emerges. 2) a dip centred at 150-200 meV BE forms. 3) the position of the hump at 500 meV BE shifts to a higher BE. The similar behaviors at different momentum positions indicate that the redistribution is independent of the details of band structures.

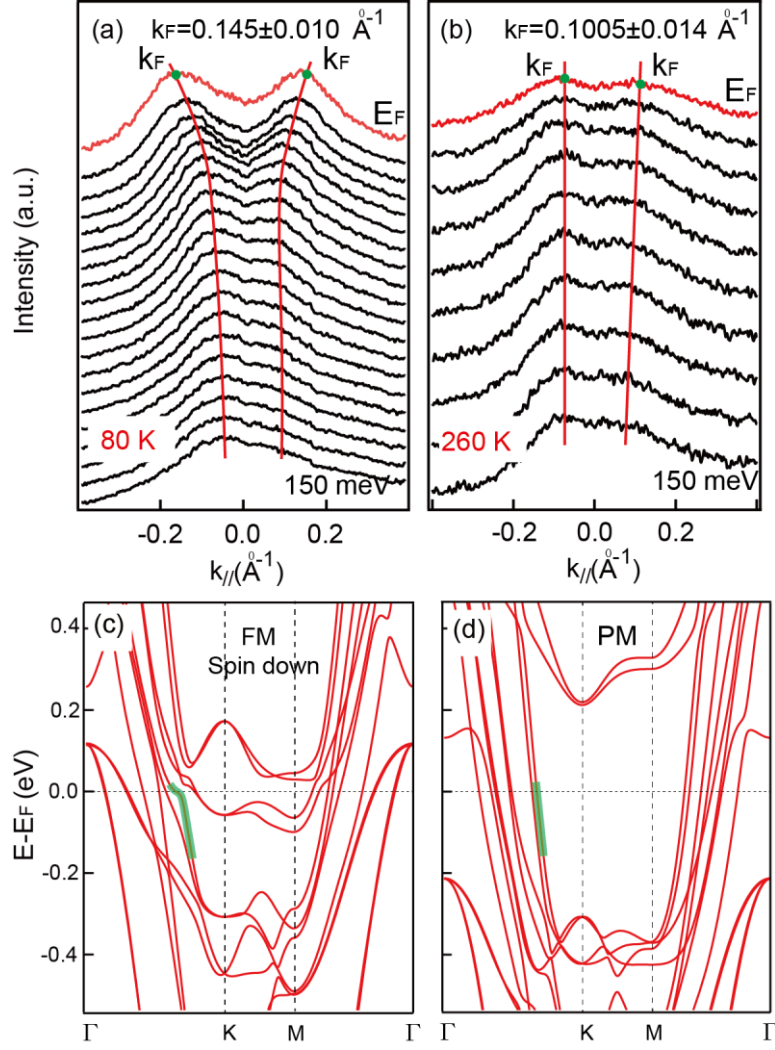


fig. S3. Enlarged Fermi surface volume in the FM state. (a and b) MDCs of band γ of FGT in the energy range from 150 meV BE to E_F at 80 K and 260 K, respectively. The red solid lines trace the peak positions of the MDCs. The Fermi vectors k_F at 80 K and 260 K of band γ are also obtained. The Fermi vectors of band γ are obtained by tracing the peak positions of the MDCs at E_F . The waterfall bands are obvious in both MDCs. (c and d) Calculated band structures of the spin down channel in the FM state and the band structures in PM state, respectively. The green bold lines mark the γ band. Exchange splitting separates spin up and spin down channels of the electronic states and shifts the hybridized part of the valence bands to E_F in fig. S3(c). The hybridization between the strongly dispersive band and weakly dispersive band near E_F enlarges the Fermi surface volume and effective electron mass. When FGT compound is in the PM state, only strong dispersive bands cross the Fermi level in fig. S3(d), consequently losing its large effective electron mass. The calculated results are in agreement with ARPES data in fig. S3(a)-(b). However, the calculation results overestimate the pocket volume of γ band.

Differently, the γ band in calculation results is an electron-like band in fig. S3(c)-(d) and fig. S5. While it looks more like a waterfall-like band in experimental results. Similar waterfall-like spectra have been observed in copper-oxide superconductors or Sr_2RuO_4 compounds (6, 55, 56). Unfortunately, there is still no consensus on the physics behind these phenomena. Up to now, several qualitative explanations have been proposed for the waterfall band, including strong coupling to a bosonic mode (57–59), strong correlations (60–63), disorder-localized band tailing (64) and photoemission matrix element (65, 66). In principle, any strong coupling to a bosonic mode leads to the appearance of the incoherent spectral weight below the energy of the mode (67), which can resemble waterfall-like band with decreased intensities. However, we believe this picture is unlikely in FGT since so far there is no known mode occurring at so large energy in Fig. 3 in the main text. Besides, the coupling to bosonic mode is a low temperature phenomena, inconsistent with the ARPES results, the spectrum of which still exhibits obvious waterfall band at 300 K.

The disorder-localized band tailing (64) is an unlikely responsible for the formation of the two branches of waterfall band, as their different morphology. The strong correlations can be an option, because the correlation-induced waterfall-like band can be observed at high temperature (63) and the waterfall connects two conduction bands (61). Matrix-element effect could be another candidate for the waterfall-like band (56). Evidently, the waterfall band represents a new phenomenon which deserves more systematic studies.

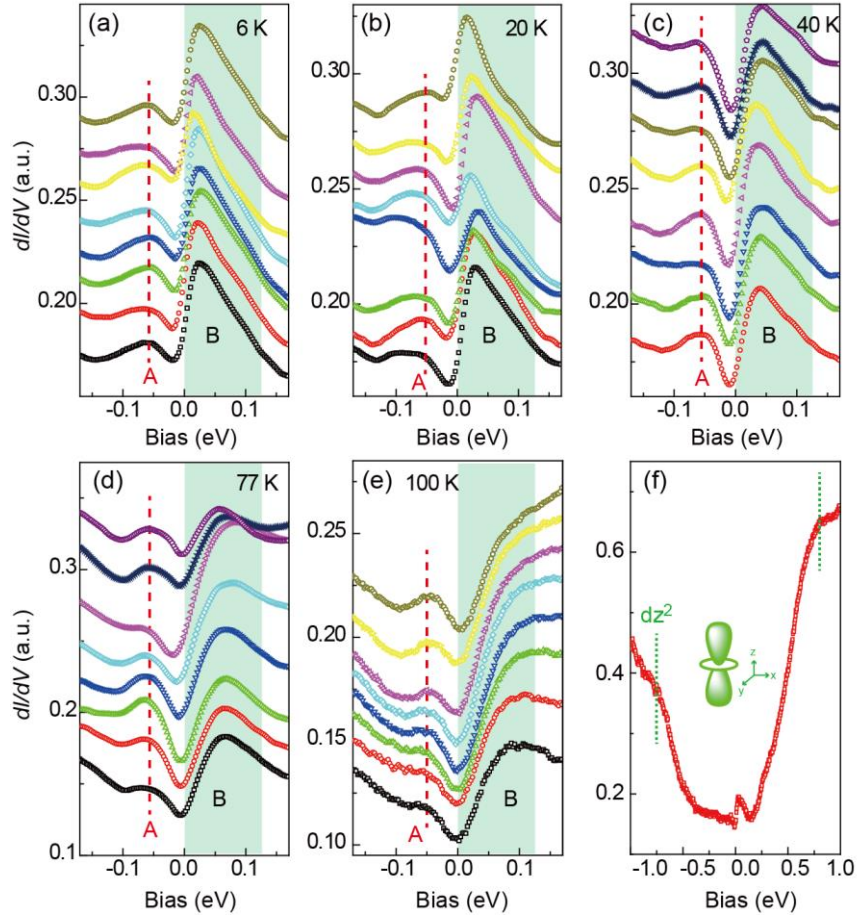


fig. S4. Spatial-resolved low-energy dI/dV spectra at different temperatures. (a to e) Partial spatial-resolved low energy dI/dV spectra measured at 6 K, 20 K, 40 K, 77 K and 100 K, respectively. The two peaks (A and B) are marked with red dashed line and green shadow, respectively. (f) High energy dI/dV spectra measured at 6 K for FGT. The green dashed lines mainly mark the Fe I d_{z^2} orbital.

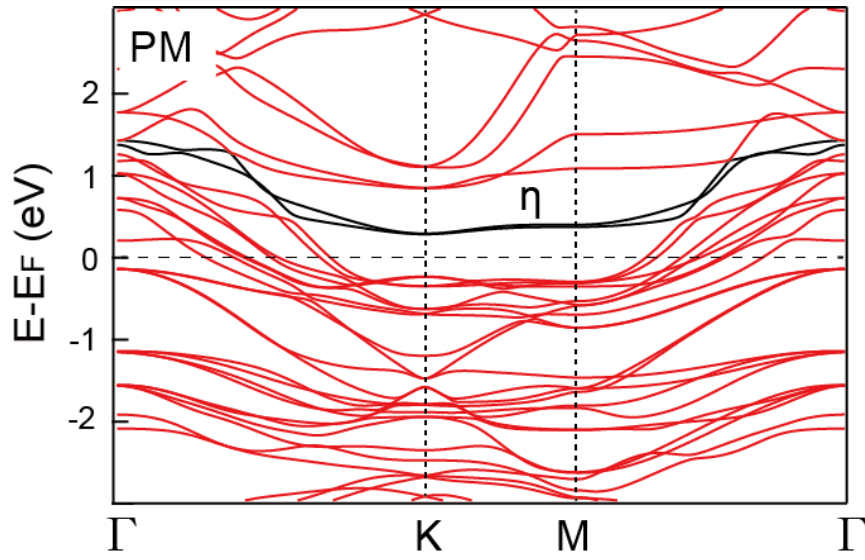


fig. S5. Band structures of Te-terminated FGT in the PM state. In the PM state, the flat bands are away from the Fermi level. While in the FM state, the exchange splitting interaction shifts flat bands to Fermi level in Fig.5 in the main text.

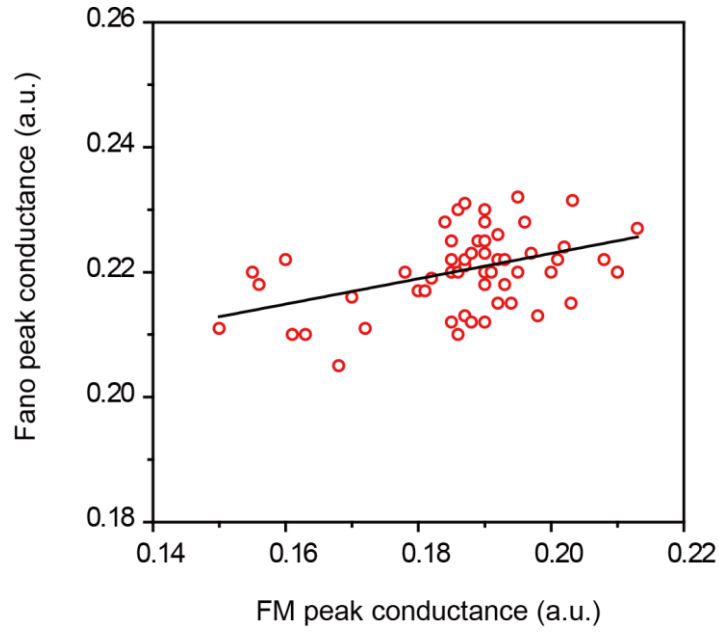


fig. S6. The positive correlation between ferromagnetism and Kondo lattice behavior. The dI/dV value at +25 mV as a function of that at -50 mV, summarized from different spatial locations of FGT at 6 K. There is an obvious positive correlation between the two quantities indicated by the linear fitting line (black line). The phenomenon is agreement with the similar distributions of the dI/dV maps at bias voltages of -50 mV and +25 mV in Fig. 4a to b in the main text. Furthermore, compared with the dI/dV values at -50 mV, the values at +25 mV exhibit small changes. The different responses to spatial locations also indicate the different origins of the two peaks.